

Theory of dressed-state lasers in the bad-cavity limit

Jakub Zakrzewski

Instytut Fizyki, Uniwersytet Jagielloński, Reymonta 4, 30-059 Kraków, Poland

Maciej Lewenstein

Institute for Theoretical Physics, Polish Academy of Sciences, Al. Lotników 32/46, 02-668 Warsaw, Poland

(Received 31 May 1991)

We present a theory of dressed-state lasers, i.e., lasers that operate on an inverted transition between dressed states of a coupled atom-field system, in the bad-cavity limit. We discuss the validity of the effective Hamiltonian approach in such a case and generalize the theory beyond secular and effective Hamiltonian approximations. We demonstrate that higher-order instabilities that lead to self-pulsing and optical chaos may occur in experiments on dressed-state lasers. With the help of the generalized theory we study the competition between the resonant one-photon and two-photon processes and try to understand it physically by looking at the spectrum of the emitted radiation.

PACS number(s): 42.50.Hz, 42.55.-f, 42.65.-k, 42.50.Lc

I. INTRODUCTION

Recently there has been a growing interest in the theoretical [1–5] and experimental [6–8] studies of dressed-state lasers, i.e., lasers that operate due to the gain on an inverted transition between dressed states of a coupled atom-field system.

The idea of a dressed-state laser stems from Mollow [9], who predicted that strongly driven homogeneous ensembles of two-level atoms can exhibit optical amplification as well as absorption. Mollow's prediction has been experimentally demonstrated in several works [10, 11].

Let us start the present discussion by reviewing physical principles on which dressed-state lasers operate. A two-level atom driven by a strong laser field of the frequency ω_L undergoes dressing [12]. If the driving frequency ω_L is detuned from the atomic transition frequency ω_a by $\Delta_1 = \omega_a - \omega_L$, while the Rabi frequency of the resonant driving field is Ω , the atom-field states form a ladder of doublets (which we denote $|+\rangle$ and $|-\rangle$), separated by ω_L and split by the generalized Rabi frequency $\Omega' = \sqrt{\Omega^2 + \Delta_1^2}$. For nonzero detuning Δ_1 , the stationary inversion of the dressed-state doublets is usually different from zero. In particular, for $\Delta_1 < 0$, the population of the upper dressed states $|+\rangle$ is larger than that of the $|-\rangle$ states. If, in this situation, one locates the ensemble of dressed atoms in an optical cavity that is resonant with transitions between $|+\rangle$ and $|-\rangle$ states of adjacent dressed-state doublets, i.e., with $\omega_c = \omega_L + \Omega'$, lasing will occur for sufficiently large atomic density. The effect of optical gain on such transitions has been studied theoretically by Holm and co-workers [13] and experimentally with confocal optical cavities by Zhu, Lezama, and Mossberg [14]. Single photon dressed-state lasing has now been observed both in atomic-vapor-cell [6] and atomic-beam [7] experiments.

Multiphoton dressed-state lasers are based on similar principles, but employ multiphoton resonances between dressed states. In a recent Letter [1] we have

demonstrated that in a system of highly driven two-level atoms located in a cavity, two-photon lasing in the optical regime should occur. Our findings were supported by experimental observation of the two-photon gain in such a system [8]. In a series of papers [2–4] (that we call I, II, and III) we have presented further developments of the theory of dressed-state lasers.

In I, we formulated the theory of dressed-state lasers using an effective Hamiltonian approach [15]. In this approach one assumes that the cavity frequency Δ_2 is in resonance with the appropriate transition frequency between the dressed states ($\Delta_2 \simeq \Omega'$ for single-photon resonance, or $2\Delta_2 \simeq \Omega'$ for two-photon resonance). The effective Hamiltonians are derived using the procedure analogous to the standard [16] or generalized [17] rotating-wave approximation. The difference is that the expansion parameter here is the ratio of coupling constant to Δ_2 or Ω' , rather than the ratio of coupling constant to optical transition frequency ω_a . The expansion parameter is thus moderately small, and one typically has to include terms in effective Hamiltonian that have the form of Stark shifts and Bloch-Siegert shifts [18]. Such terms distinguish the theory of dressed-state lasers from the standard laser models [19], and may influence stability properties of the dressed-state lasers. In Refs. [1] and [2] we have compared the theories of one-photon and two-photon dressed-state lasers to discuss the competition between one-photon and two-photon regimes of operation. Fortunately, the regions of operation of one-photon and two-photon lasers are often distinct, especially for good cavities characterized by a small width Γ . Therefore, prospects for an experimental observation of the optical two-photon laser are good. Resonant two-photon processes, although generally speaking characterized by a smaller coupling, will not be destroyed by competing, but nonresonant single-photon processes.

In the subsequent paper, II, we have demonstrated that nonresonant transitions between dressed states that lead to the appearance of Stark and Bloch-Siegert shifts also affect quantum properties of emitted radiation. In

fact, both single-photon and two-photon dressed-state lasers are predicted to exhibit squeezing [20]. Squeezing occurs in the regions of parameter space not far from the lasing threshold and is correlated to an appearance of larger Bloch-Siegert and Stark shifts. Large squeezing effects (60% reduction of the relative variance of the field quadrature) are possible when atom-cavity coupling is large and the cavity is not too narrow. Finally, we should mention that squeezing is practically not affected by pump-depletion effects [4].

Until now two possibilities of an experimental realization of dressed-state lasers have been considered: (i) the use of confocal cavities [7] that are characterized by high values of atom-cavity coupling g ; (ii) the use of standard Fabry-Pérot cavities that can be very narrow. The first case is, in our opinion, much more interesting, since it may lead to large squeezing. On the other hand, for such cavities, the system is typically not far from the bad-cavity limit, i.e., the limit when cavity width is larger than any other width characterizing the system. Obviously, for Fabry-Pérot cavities, the bad-cavity limit is also easy to be realized experimentally. Lasing in such a case may still be possible, since to reduce the effect of the large cavity width one may increase the number of atoms in the cavity.

On the other hand, it is known that in the bad-cavity limit standard laser theory of the single-mode laser with homogeneous broadening predicts higher-order instabilities such as self-pulsing and chaos (see, for instance, Ref. [19]). It is interesting, therefore, to investigate possibilities of such instabilities for dressed-state lasers.

In the present paper we address and attempt to resolve two fundamental problems of the theory of dressed-state lasers.

(i) *The emergence of self-pulsing and chaos.* The theory presented in Refs. [2–4], as well as in the papers of Agarwal [5] was based on an effective-Hamiltonian approach and the so-called secular approximation. The latter approximation consists in taking into account only resonant spontaneous transitions between dressed states. Even within this framework and in the parameter region of its validity (see Secs. II and III) the presence of Bloch-Siegert shifts and Stark shifts may enhance the significance of higher-order instabilities (i.e., of self-pulsing and chaos). We identify the regions of parameters where higher instabilities occur and see how far they are from experimentally accessible situations. The results that are obtained in the regions of validity of effective Hamiltonian theory are discussed in Sec. IV.

(ii) *Generalization of the theory beyond secular and effective-Hamiltonian approach.* The effective-Hamiltonian approach may alternatively be interpreted as a kind of adiabatic approximation. It is in fact equivalent to performing the following procedure: First, we write the full set of equations describing the evolution of the system. Second, we identify appropriate macroscopic variables that describe the process in question (cavity field, dressed-state inversion and dressed-state polarizations). The number of relevant macroscopic variables is always finite. Third, we write the equations for macroscopic variables and eliminate adiabati-

cally the remaining variables from these equations. When such an adiabatic elimination is performed neglecting spontaneous-emission terms, one obtains the same result as in the effective-Hamiltonian approach with the secular approximation. Full elimination allows one to go beyond the secular approximation. Effective-Hamiltonian theory (EHT) described in terms of adiabatic elimination and generalization beyond secular approximation (effective adiabatic theory, EAT) are discussed in Sec. II. To go beyond the secular approximation we introduce the whole hierarchy of macroscopic variables, and perform the adiabatic elimination by breaking the hierarchy on the higher level. Such a procedure allows for systematic improvements of the effective-Hamiltonian theory. The hierarchy of macroscopic polarizations and generalized “effective” approach (GET) are presented in Sec. III.

In the present paper we discuss the results that correspond to up to 41 appropriately chosen macroscopic variables. We compare the results for such an improved “effective” theory with the standard effective-Hamiltonian approach. In this way we answer a part of the first question, i.e., we identify the regions of validity of the effective-Hamiltonian approach. We show, on the other hand, that for bad cavities secular approximation may break down, despite the fact that the spontaneous emission rate is the slowest rate in the system. In the bad-cavity limit the system becomes, generally speaking, more unstable, and consequently the effective-Hamiltonian approach (with or without the secular approximation) becomes very inaccurate. In particular, the competition between one-photon and two-photon processes may lead to self-pulsing and chaotic behavior, which cannot be predicted within the effective-Hamiltonian framework. The results in the region where the effective-Hamiltonian approach is not valid are discussed in Sec. V.

Our aim is to illustrate what kind of differences between full theory and effective-Hamiltonian theory arise, and to discuss the details of the competition between one-photon and two-photon processes. We also try to understand the competition in a quantitative and physical sense by looking at the spectrum of the emitted radiation.

We stress that our theory and the physical problem that we study are very closely related to the works on multimode instability of optical bistability, initiated by Bonifacio and Lugiato [21] and carried on over the years (for a recent review see Ref. [22]). These papers were in fact the first to demonstrate that Mollow gain [9] can induce cavity lasing. The theoretical results of Brambilla *et al.* [22] have found a very precise confirmation in a series of nice experiments by Segard *et al.* ([23], see also [24]).

The main difference between our work and previous theoretical studies is the fact that the latter consider the standard problem of optical bistability. The input field pumps one of the cavity modes of similar frequency. Under appropriate conditions, the interaction between the pump mode and the atoms can create Mollow gain for one or several cavity modes close to the resonance. When this gain overcomes losses these modes exhibit laser action. *The conditions considered by us differ, because in*

our case the input field does not pump cavity modes. In addition, four-wave-mixing effects are avoided in our theory, contrary to the case of optical bistability.

II. EFFECTIVE ADIABATIC AND EFFECTIVE-HAMILTONIAN THEORIES

In the previous works [1–4] effective Hamiltonians for dressed-state lasers were constructed using the method of Stenholm [15], which in fact is a version of time-independent second-order perturbation theory. We have applied such a perturbative approach only to the Hamiltonian. In the spontaneous decay terms in the Liouvilian, the so-called secular approximation was used, i.e., only resonant spontaneous transitions between dressed states were considered. To go beyond secular approximation we reformulate here our theory in terms of the adiabatic elimination procedure applied to semiclassical equations of motion.

As in I, II, and III we consider a system of N two-level atoms located in a cavity. The atoms are pumped by an external driving field of frequency ω_L . The strength of the pump is characterized by the Rabi frequency Ω . The pumping field has a traveling-wave character and is oriented orthogonal to the cavity modes.

Let $\sigma_{3\mu}$, σ_μ^\dagger , and σ_μ denote the standard Pauli matrices that describe two-level atoms, each of which is enumerated by an index μ . The atoms interact with the pumping field and with a single, nearly resonant mode of the cavity. Let us denote the cavity-photon creation and annihilation operators by a^\dagger and a . Additionally, the atoms may undergo spontaneous emission into the modes of the electromagnetic field that are not associated with the cavity resonance. The density matrix of the system then obeys the Liouville–von Neumann (master) equation of the form [25]

$$\dot{\rho} = -i[\mathcal{H}, \rho] + \mathcal{L}_{AP} + \mathcal{L}_{FP} . \quad (2.1)$$

The Hamiltonian in Eq. (2.1) is in the standard rotating-wave approximation given by the expression

$$\begin{aligned} \mathcal{H}' = & \sum_{\mu} \frac{\Omega'}{2} \sigma_{3\mu} + \Delta_2 a^\dagger a + \sum_{\mu} \frac{g_{\mu}^*}{4} a^\dagger [(1 + \cos 2\alpha) \sigma_{\mu} - (1 - \cos 2\alpha) \sigma_{\mu}^\dagger + \sin(2\alpha) \sigma_{3\mu}] \\ & + \sum_{\mu} \frac{g_{\mu}}{4} [(1 + \cos 2\alpha) \sigma_{\mu}^\dagger - (1 - \cos 2\alpha) \sigma_{\mu} + \sin(2\alpha) \sigma_{3\mu}] a . \end{aligned} \quad (2.7)$$

The spontaneous-emission term (2.4) in the dressed-states basis is

$$\begin{aligned} \mathcal{L}_{AP} = & \frac{\gamma}{2} \sum_{\mu} \{ [\sin(2\alpha) \sigma_{3\mu} + (1 + \cos 2\alpha) \sigma_{\mu} - (1 - \cos 2\alpha) \sigma_{\mu}^\dagger] \rho [\sin(2\alpha) \sigma_{3\mu} + (1 + \cos 2\alpha) \sigma_{\mu}^\dagger - (1 - \cos 2\alpha) \sigma_{\mu}] \\ & - [1 + \sigma_{3\mu} \cos 2\alpha - (\sigma_{\mu} + \sigma_{\mu}^\dagger) \sin 2\alpha] \rho - \rho [1 + \sigma_{3\mu} \cos 2\alpha - (\sigma_{\mu} + \sigma_{\mu}^\dagger) \sin 2\alpha] \} . \end{aligned} \quad (2.8)$$

$$\begin{aligned} \mathcal{H} = & \frac{1}{2} \sum_{\mu}^N [\Delta_1 \sigma_{3\mu} + \Omega(\sigma_{\mu} + \sigma_{\mu}^\dagger) + g_{\mu} \sigma_{\mu}^\dagger a + g_{\mu}^* a^\dagger \sigma_{\mu}] \\ & + \Delta_2 a^\dagger a . \end{aligned} \quad (2.2)$$

The free parts of the Hamiltonian, corresponding to the first and the last terms in Eq. (2.2), are proportional to the appropriately defined detunings $\Delta_1 = \omega_a - \omega_L$ and $\Delta_2 = \omega_c - \omega_L$. The term proportional to the Rabi frequency Ω describes the driving of the atoms, while the coefficients g_{μ} denote the coupling of the atom μ to the cavity mode. The phases of individual atomic dipoles are fixed relative to the pump field in the expression (2.2), and by that a spatially varying phase ϕ_{μ} is introduced into g_{μ} 's. The magnitude of the atom-cavity coupling constant, on the other hand, is assumed to be a constant, i.e., $|g_{\mu}| = g \exp(i\phi_{\mu})$ (for a detailed discussion, see I).

The last two terms in Eq. (2.1) describe cavity damping and spontaneous emission, i.e.,

$$\mathcal{L}_{FP} = 2\Gamma(a\rho a^\dagger - \frac{1}{2}a^\dagger a\rho - \frac{1}{2}\rho a^\dagger a) \quad (2.3)$$

and

$$\mathcal{L}_{AP} = 2\gamma \sum_{\mu} (\sigma_{\mu} \rho \sigma_{\mu}^\dagger - \frac{1}{2} \sigma_{\mu}^\dagger \sigma_{\mu} \rho - \frac{1}{2} \rho \sigma_{\mu}^\dagger \sigma_{\mu}) , \quad (2.4)$$

where Γ is the cavity half width at half maximum and 2γ denotes the free-space atomic-spontaneous-emission rate.

Equations (2.1)–(2.4) are written in the basis of the atomic Hilbert space, consisting of bare excited states $|1\rangle_{\mu}$ and bare ground states $|0\rangle_{\mu}$. To obtain a dressed-state picture, we change the basis, introducing dressed states [12]

$$|+\rangle_{\mu} = \cos \alpha |1\rangle_{\mu} + \sin \alpha |0\rangle_{\mu} \quad (2.5)$$

and

$$|-\rangle_{\mu} = -\sin \alpha |1\rangle_{\mu} + \cos \alpha |0\rangle_{\mu} . \quad (2.6)$$

In the above expressions the “rotation” angle α , which belongs to the interval $[0, \pi/2]$, is defined through the relations $\Omega = \Omega' \sin 2\alpha$ and $\Delta_1 = \Omega' \cos 2\alpha$, where Ω' denotes an effective Rabi frequency, equal to the dressed-state energy splitting $\Omega' = \sqrt{\Omega^2 + \Delta_1^2}$.

After elementary calculations, we obtain the explicit form of the Hamiltonian transformed to the dressed basis

In Eqs. (2.7) and (2.8) the symbols $\sigma_{3\mu}$, σ_μ^\dagger , and σ_μ refer to the atomic operators in the dressed-state basis, and correspond to the dressed-state inversion, raising, and lowering operators, respectively. The cavity damping term (2.3) remains unchanged under the change of basis of Eqs. (2.5) and (2.6).

From the expressions (2.7) and (2.8), and (2.3) we derive the equation of motion for the quantum-mechanical averages σ_μ , σ_μ^\dagger , $\sigma_{3\mu}$, a , and a^\dagger . Anticipating a semiclassical approximation, we may treat these equations as classical c -number equations (i.e., we decorrelate atom-cavity-field products). To do so we introduce the notation

$$\begin{aligned}\gamma_0 &= \gamma \sin 2\alpha, \\ \gamma_1 &= \frac{\gamma}{2}(2 + \sin^2 2\alpha), \\ \gamma_2 &= \gamma(1 + \cos^2 2\alpha), \\ \gamma_3 &= \frac{\gamma}{2} \sin 2\alpha \cos 2\alpha, \\ \gamma_4 &= \frac{\gamma}{2} \sin^2 2\alpha,\end{aligned}\quad (2.9)$$

and

$$F_\pm = \frac{g}{4}(1 \pm \cos 2\alpha), \quad F_0 = \frac{g}{4} \sin 2\alpha. \quad (2.10)$$

The equations of motion take then the form

$$\begin{aligned}\dot{\sigma}_\mu &= -(\gamma_1 + i\Omega')\sigma_\mu + \gamma_0 + \gamma_3\sigma_{3\mu} - \gamma_4\sigma_\mu^* \\ &\quad + ie^{i\phi_\mu} F_+ \sigma_{3\mu} a - ie^{-i\phi_\mu} F_- a^* \sigma_{3\mu} \\ &\quad - 2iF_0(e^{-i\phi_\mu} a^* \sigma_\mu + e^{i\phi_\mu} \sigma_\mu a),\end{aligned}\quad (2.11)$$

$$\begin{aligned}\dot{\sigma}_{3\mu} &= -\gamma_2(\sigma_{3\mu} - \bar{\sigma}_{3\mu}) + 2\gamma_3(\sigma_\mu + \sigma_\mu^*) \\ &\quad + 2iF_+(e^{-i\phi_\mu} a^* \sigma_\mu - e^{i\phi_\mu} \sigma_\mu^* a) \\ &\quad + 2iF_-(e^{-i\phi_\mu} a^* \sigma_\mu^* - e^{i\phi_\mu} \sigma_\mu a),\end{aligned}\quad (2.12)$$

$$\dot{a} = -(\Gamma + i\Delta_2)a - i \sum_\mu e^{-i\phi_\mu} (F_+ \sigma_\mu - F_- \sigma_\mu^* + F_0 \sigma_{3\mu}). \quad (2.13)$$

The equations for σ_μ^* , and a^* are the complex conjugates of (2.11) and (2.13), respectively.

To formulate the dressed-state-laser theory we identify the macroscopic variables that are the relevant order parameters for each type of lasing. Here we shall present detailed calculations for the case of the one-photon dressed-state laser. For such a case the relevant macroscopic variables are for the dressed-state polarization,

$$S = \sum_\mu e^{-i\phi_\mu} \sigma_\mu, \quad (2.14)$$

and its conjugate S^* ; and for the dressed-state inversion,

$$S_3 = \sum_\mu \sigma_{3\mu}; \quad (2.15)$$

the cavity field amplitude a , and its conjugate a^* .

We introduce also the stationary dressed-state inversion $\bar{S}_3 = \sum_\mu \bar{\sigma}_{3\mu}$. From Eqs. (2.11) and (2.12) it is elementary to derive equations of motion for the macroscopic variables. Such equations, of course, contain on the right-hand side couplings to combinations of σ_μ and $\sigma_{3\mu}$ other than S , S^* , S_3 . On the other hand, each of the Eqs. (2.11) and (2.12) contains on the right-hand side couplings to S , S^* , S_3 apart from couplings to other terms. The latter can be neglected in the lowest-order. One can solve then Eqs. (2.11) and (2.12) adiabatically, expressing σ_μ , σ_μ^\dagger , and $\sigma_{3\mu}$ in terms of S , S^* , S_3 . The solutions are then inserted into the equation of motion for the macroscopic variables and averaged over spatially varying phases ϕ_μ (for the discussion of the latter point see I). The resulting closed set of nonlinear equations represents what we call in the following the effective-adiabatic theory (EAT). These equations are expected to be valid close to resonance, $\Delta_2 = \Omega'$. They include systematically the terms of order of $[F^2/(\Omega'$ or $\Delta_2)]$, $(F\gamma/\Omega')$, or γ^2/Ω' , etc. The equations of the EAT read:

$$\begin{aligned}\dot{S} &= -(\gamma_1 + i\Omega')S + iF_+ S_3 a - \left[\frac{2iF_-^2}{\Omega' + \Delta_2 + i\gamma_2} - 4iF_0^2 \left(\frac{1}{\Omega' - i\gamma_1} - \frac{1}{\Delta_2 + i\gamma_1} \right) \right] S a^* a \\ &\quad + \left(\frac{2i\gamma_3^2}{\Omega' + i\gamma_2} - \frac{i\gamma_4^2}{\Omega' + \Delta_2 + i\gamma_1} \right) S + \left(\frac{\gamma_4 F_- S_3}{\Omega' + \Delta_2 + i\gamma_1} - \frac{2F_0(\gamma_0 N + \gamma_3 S_3)}{\Omega' - i\gamma_1} \right) a,\end{aligned}\quad (2.16)$$

$$\begin{aligned}\dot{S}_3 &= -\gamma_2(S_3 - \bar{S}_3) + 2iF_+(a^* S - S^* a) - 4F_0\gamma_3 \left(\frac{a^* S}{\Omega' - i\gamma_1} + \frac{S^* a}{\Omega' + i\gamma_1} \right) + \frac{4\gamma_1\gamma_3}{\Omega'^2 + \gamma_1^2} (\gamma_0 N + \gamma_3 S_3) \\ &\quad - \frac{4\gamma_1 F_-^2}{(\Omega' + \Delta_2)^2 + \gamma_1^2} S_3 a^* a + 2\gamma_4 F_- \left(\frac{a^* S}{\Omega' + \Delta_2 + i\gamma_1} + \frac{S^* a}{\Omega' + \Delta_2 - i\gamma_1} \right),\end{aligned}\quad (2.17)$$

$$\dot{a} = -(\Gamma + i\Delta_2)a - iF_+ S - \frac{iF_-^2 S_3 a}{\Omega' + \Delta_2 + i\gamma_1} + \frac{\gamma_4 F_- S}{\Omega' + \Delta_2 + i\gamma_1} + \frac{2\gamma_3 F_0 S}{\Omega' + i\gamma_2}. \quad (2.18)$$

The above equations are expected to be valid for the well-defined resonance when both Ω' and Δ_2 are much larger than γ and F . In such situations it is natural to neglect terms proportional to γ in the adiabatic denominators in Eqs. (2.16), (2.17), and (2.18). The terms containing adiabatic denominators and proportional to γ originate from the non-Hamiltonian part of the evolution. The secular approximation (which is valid when γ is sufficiently small) consists of neglecting all those terms, that is, the last four terms in Eq. (2.16), the last four terms in Eq. (2.17), and the last two terms in Eq. (2.18).

After performing secular approximation we obtain a set of equations that are fully equivalent to the one derived with the help of the effective Hamiltonian (see I). The equations of the effective-Hamiltonian theory (EHT) thus read:

$$\dot{S} = -(\gamma_1 + i\Omega')S + iF_+ S_3 a - \frac{2iF_-^2}{\Omega' + \Delta_2} S^* a, \quad (2.19)$$

$$\dot{S}_3 = -\gamma_2(S_3 - \bar{S}_3) + 2iF_+(a^* S - S^* a), \quad (2.20)$$

$$\dot{a} = -(\Gamma + i\Delta_2)a - iF_+ S - \frac{iF_-^2 S_3 a}{\Omega' + \Delta_2} \quad (2.21)$$

The above equations have been thoroughly studied in I, II, and III. Note that the same procedure is applicable for two-photon resonance, when $2\Delta_2 \simeq \Omega'$. The only difference is that the appropriately defined macroscopic polarization variable for two-photon lasing is

$$S = \sum_{\mu} e^{-2i\phi_{\mu}} \sigma_{\mu}. \quad (2.22)$$

Using the definition (2.22) one can derive equations of two-photon EAT and EHT. The latter are fully equivalent to the one studied in I, II, and III.

Note, that EAT equations have typically much more complicated structure than EHT equations. Contrary to the case of EHT, we were not able to find stationary solutions of EAT equations analytically. Again we remind the reader that the EHT method, as compared to the EAT method, should work for small γ . Our results indicate quite generally that the bigger the dressed-state splitting is, the better the EHT method works. For strongly unstable regimes, however, we may expect qualitative and quantitative differences between the two theories even for small γ . For instance, close to the threshold of instabilities, the EAT method works usually much more accurately than the EHT method. A detailed discussion of the validity of both approaches will be presented in Secs. IV and V. First we have to formulate the method of systematic improvement to the approximations used. Such a method, based on an introduction of the whole hierarchy of macroscopic order parameters will be presented in Sec. III.

III. GENERALIZED EFFECTIVE THEORIES (GET)

One of the basic problems that one encounters when using EAT or EHT methods is the competition between

one-photon and two-photon processes. The information about the stability of one-photon and two-photon dressed-state lasers comes from two distinct theories. Each of them describes the evolution of a different set of macroscopic variables. In particular, macroscopic polarizations for one-photon and two-photon lasing are entirely different [compare Eqs. (2.14) and (2.22)]. The competition problem may be in such distinct theories studied only in the stationary limit. It is natural then to ask for the theory that would simultaneously describe the dynamics of both kinds of lasing processes. One should in such theories introduce both the one-photon polarization (2.14), as well as the two-photon one (2.22). This idea led us to the formulation of generalized effective theories that are based on a hierarchy of macroscopic variables.

We introduce the following hierarchy of macroscopic variables.

(i) The family of n -photon polarizations that describe multiphoton transitions between the dressed states,

$$S^{(n)} = \sum_{\mu} e^{-in\phi_{\mu}} \sigma_{\mu}. \quad (3.1)$$

The polarizations with $n > 0$ ($n < 0$) build up in n -photon lasing processes that correspond to the transitions from the upper (lower) to the lower (upper) dressed states, respectively. The $n = 0$ polarization corresponds to the coherence linking dressed states of the same doublet.

(ii) The family of complex conjugates of $S^{(n)}$,

$$S^{(n)*} = \sum_{\mu} e^{in\phi_{\mu}} \sigma_{\mu}^*. \quad (3.2)$$

(iii) The family of polarizations that correspond to n -photon transitions from both lower to lower and higher to higher dressed states. We call such transitions n th-order Rayleigh transitions, since they lead to the emission at the driving laser frequency,

$$S_3^{(n)} = \sum_{\mu} e^{-in\phi_{\mu}} \sigma_{3\mu}. \quad (3.3)$$

Note that $S_3^{(-n)} = S_3^{(n)*}$ and that S_3^0 is the dressed-state inversion (2.15).

Similar variables for the single-atom case (apart for the phase factor) has been defined by Grynberg, Pinard, and Verkerk [26] in their discussion of saturation four-wave mixing. They used the quantum-dressed-state approach in the Schrödinger picture in which, e.g., $S_3^{(n)}$ corresponds to the reduced [27] coherence

$$\begin{aligned} \Delta^{(n)} = & \sum_K \langle K + n, + | \rho | K, + \rangle \\ & - \langle K + n, - | \rho | K, - \rangle. \end{aligned} \quad (3.4)$$

The approach used in Ref. [26] for the four-wave-mixing problem neglected all nonresonant coupling and was, therefore, equivalent, to the GET5 approach (see below).

From Eqs. (2.11), (2.12), and (2.13) it is elementary to derive equations of motion for the hierarchy of macroscopic variables,

$$\begin{aligned} \dot{S}^{(n)} = & -(\gamma_1 + i\Omega')S^{(n)} + iF_+ S_3^{(n-1)}a - iF_- a^* S_3^{(n+1)} \\ & - 2iF_0(a^* S^{(n+1)} + aS^{(n-1)}) \\ & + \gamma_0 N \delta_{n0} + \gamma_3 S_3^{(n)} - \gamma_4 S^{(-n)*}, \end{aligned} \quad (3.5)$$

$$\begin{aligned} \dot{S}_3^{(n)} = & -\gamma_2(S_3^{(n)} - \bar{S}_3 \delta_{n0}) + 2iF_+(a^* S^{(n+1)} - aS^{(-n+1)*}) \\ & + 2iF_-(a^* S^{(-n-1)*} - aS^{(n-1)}) \\ & + 2\gamma_3(S^{(n)} + S^{(-n)}) \end{aligned} \quad (3.6)$$

that, together with the equation for the field amplitude Eq. (2.13) rewritten as

$$\dot{a} = -(\Gamma + i\Delta_2)a - iF_+ S^{(1)} + iF_- S^{(-1)*} - iF_0 S_3^{(1)}, \quad (3.7)$$

form a closed albeit infinite set of equations.

To solve this hierarchy of equations, we propose to break it in a systematic way. The starting point again will be the theory of the one-photon dressed-state laser. In lowest order we simply write down the equations for the five relevant variables ($S^{(1)}$, $S^{(1)*}$, $S_3^{(0)}$, a , and a^*) and neglect all the couplings of these variables to any other macroscopic variables. In this way we obtain generalized effective theory with five equations (GET5). Such a theory is in fact equivalent to neglecting all terms that come from adiabatic elimination in Eqs. (2.19), (2.20), and (2.21). In other words, such a theory corresponds to neglecting all antiresonant terms in the dressed-state Hamiltonian (2.7), and is equivalent to the EHT approach in which Bloch-Siegert shifts are neglected and secular approximation is made. This simplified theory serves quite well for estimations of lasing thresholds (see Ref. [1]).

The next step is to include in the theory those macroscopic variables that appear on the right-hand side of the exact equations for the first five variables. All other macroscopic variables are neglected. There are ten new variables that enter the right-hand side of the five equations of GET5. We call the resulting theory GET15.

The further systematic improvements of the theory are constructed similarly. Having a theory with m variables, GET m , we identify m' new variables that enter the right-hand side of the m exact equations for m variables. We include these and only these m' new variables into the improved theory, GET($m + m'$). We write the exact equations for the first m variables and the approximate equations for the m' new variables, neglecting couplings to all variables not included in the theory.

Such an approach has led us to the hierarchy of approximate theories, GET5, GET15, GET23, GET29, GET35, GET41, etc. For instance, for GET41, which was the highest we investigated, the relevant variables are $S^{(n)}$ for $n = -6, -5, \dots, 6$, its conjugates, $S_3^{(n)}$ for $n = -6, -5, \dots, 6$, and two field variables a and a^* .

The physical meaning of the breakdown of the hierarchy is the following: at each level of the approximate theory we neglect some higher-order multiphoton processes that lead to multiphoton macroscopic polarization

and lasing. To solve the equations of motion for GET theories we have used numerical methods. Solutions of equations of motion were obtained with the help of the International Mathematics and Scientific Library procedure DGEAR.

As the initial conditions we typically assumed vanishing atomic polarizations and the dressed-state inversion corresponding to atoms in their ground states, i.e., $S_3^{(0)} = -N \operatorname{sgn}(\Delta_1)$. As in our semiclassical approach quantum fluctuations are absent; we have to introduce some photons into the cavity, at least initially, to assure a possibility of a nontrivial solution for the field amplitude. Thus we assumed that $N_{\text{in}} = |a(0)|^2 > 0$.

Comparison of the results obtained for subsequent GET theories allowed us to determine the convergence of our method. It is worth stressing that in all cases studied GET41 gave qualitatively the same results as GET35 for regular trajectories and qualitatively the same for chaotic trajectories. That means that the results obtained for GET41 may be considered as “exact” in the considered regime of parameters.

In principle analogous hierarchy of generalized effective theories may be formulated without transforming to the dressed-state basis. Of course, the resulting hierarchy is not equivalent to the one considered here. We think that it is important to stress, that at least for the wide class of problems related to dressed-state lasers (i.e., to the strongly driven atomic system), the method based on dressed states seems to be much more efficient. With this method we have achieved the convergence on the level of 41 equations in the worst cases. The method based on bare states, when applied to the description of chaotic behavior, did not converge even when more equations were used.

By comparing with the “exact” results obtained with the help of GET41 we were able to check the validity of the effective-Hamiltonian and effective-adiabatic approach. The results of our studies are presented in Secs. IV and V. The results in Sec. IV are obtained in the region of parameters where both EAT and EHT are valid. The results in Sec. V illustrate the breakdown of the adiabatic approach. They are still, however, obtained in the region of validity of the generalized effective theory GET41.

IV. RESULTS IN THE REGIONS OF VALIDITY OF EFFECTIVE THEORY

Let us start the discussion by defining approximately the regime of parameters of interest. We shall use the spontaneous emission rate γ as the frequency unit and express all other parameters in terms of γ . First, we shall be approaching the bad-cavity limit, i.e., cavity width will be typically of the order of 20–100. The characteristic values of the Rabi frequency Ω depend on the intensity of the driving field. To achieve large separation of the dressed states we shall use Ω of the order of 10–100. For similar reasons, atom-laser detuning will range from 10 to 100. Finally, the atom-cavity coupling g and number of atoms N depend on the particular experiment we have in mind, i.e., experiment with confocal cavities or Fabry-

Pérot cavities. By rescaling the variables as $\tilde{a} = a/\sqrt{N}$, $\tilde{S}^{(n)} = S^{(n)}$, and $\tilde{S}_3^{(n)} = S_3^{(n)}$ one notices immediately that the relevant parameter that characterizes laser operation is in fact the product $D = g\sqrt{N}$, which for both kinds of cavities may range between 0 and a few hundred.

The first set of results we present corresponds to the situation when both EAT and EHT are valid. We have determined the regions of parameters where this takes place by comparing the results to the ones obtained with the help of the “exact” theory GET41. In particular, adiabatic theories work well for large atom-laser detuning Δ_1 .

As might be expected from the standard laser theory even a simple EHT leads to self-pulsing and chaos. We illustrate this statement in Fig. 1, which shows the instability regions in the Δ_2 - Ω' plane. For a one-photon laser for a sufficiently large value of the parameter $D = g\sqrt{N}$, a region of instability arises close to resonance ($\Delta_2 = \Omega'$). In this region the standard stationary solution above threshold becomes unstable. This region is well separated from the region of existence of the two-photon laser that is determined from the EHT theory based on the effective two-photon Hamiltonian.

We have traced the route to chaos following the pass into the instability region indicated by the vertical arrow in Fig. 1. We have observed the period-doubling route and illustrated it in Figs. 2(a)-2(f), which show

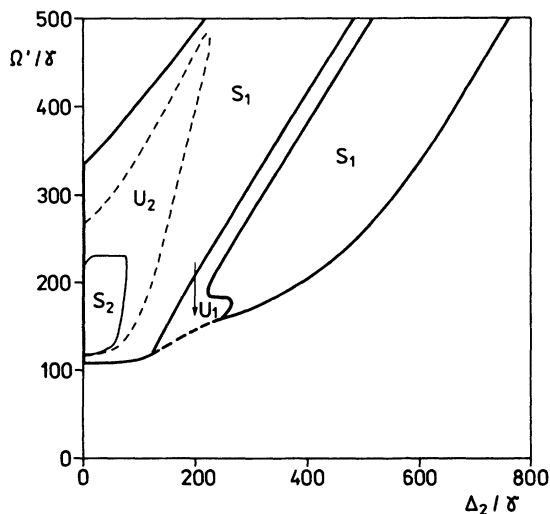


FIG. 1. Regions of existence and stability of different modes of operation of one-photon and two-photon dressed state lasers. The diagram is presented in the Δ_2 - Ω' plane and has been obtained with the help of EHT theory. Inside the large region (denoted S_1) surrounded by the solid line stationary and stable solution for the one-photon laser exist. A narrow region (U_1) close to the resonant line $\Delta_2 = \Omega'$ corresponds to the unstable one-photon laser solution with self-pulsing or chaotic behavior. Small regions on the left surrounded by dashed (U_2) and solid (S_2) lines correspond to the unstable and stable regions of stationary two-photon lasing. These curves were calculated with the help of two-photon EHT. Other parameters are $\Delta_1 = -100$, $\Gamma = 20$, $g = 0.001$, $N = 3 \times 10^{11}$. The vertical arrow indicates the route to chaos illustrated in Fig. 2

trajectories in the phase space and time dependencies. Cavity width is moderately large here, $\Gamma = 20$. As we mentioned, in this region of parameters more accurate theories give similar results. This is illustrated in the series of Figs. 3(a)-3(c), that are calculated for the values of Ω' and Δ_2 chosen in the self-pulsing region and the larger value of Γ . It is shown that the theory without secular approximation does not differ very much from the effective-Hamiltonian theory. The generalized effective theory GET41 leads to small changes in the behavior, and introduces chaotic transients [Fig. 3(c)]. The stationary state in all three cases, however, is practically the same, and can be accurately described in the framework of the simplest of those theories, i.e., EHT.

The second type of results that we present concerns the possibility of experimental observation of higher-order instabilities in dressed-state lasers. Note that when atom-laser detuning is smaller, the results of I indicate that the role of Bloch-Siegert shifts becomes more pronounced. The presence of these terms leads to the difference between one-photon dressed-state laser theory and the standard laser case. In particular, it may affect the stability properties of the dressed-state laser. Therefore, in those regions of small and moderate Δ_1 we study the stability of stationary solutions and the role of Bloch-Siegert shifts. We compare the results obtained in the framework of one-photon EHT, and GET5 (which is the same as EHT, but with Bloch-Siegert shifts neglected, i.e., it corresponds to the standard laser theory).

For the choice of parameters that corresponds to the experiment of Lezama *et al.* [7] (i.e., for not too large Δ_1), the effects of the Bloch-Siegert shifts are not very pronounced (Fig. 4). They lead only to a small increase of the size of regions of higher-order instabilities close to the resonance, $\Delta_2 = \Omega'$. Note, however, the factor 3 increase of the parameter D allows for achieving the instability region.

In the region of parameters corresponding to experiments of Lezama *et al.*, but for a slightly larger magnitude of Δ_1 , antiresonant couplings that lead to Bloch-Siegert shifts deform dramatically the stability regions (Fig. 5). Here, self-pulsing and chaos should be accessible for the value of D only two times larger than the one required to pass the threshold for stationary laser action.

The results of Figs. 4 and 5 indicate that higher-order instability region lies not too far from experimentally accessible regimes. That is a very important conclusion, since it is interesting from the fundamental point of view, and it might be extremely useful for analyzing experimental results.

V. BREAKDOWN OF ADIABATIC THEORIES

In this section we present the results in the region where EHT and EAT are not valid. There are two kinds of discrepancies between the adiabatic and “exact” theories.

First, note that the results of Sec. IV are in the region of validity of the EHT theory. They are, however, typically not valid close to the boundaries of instability region in the parameter space. The reason is that im-

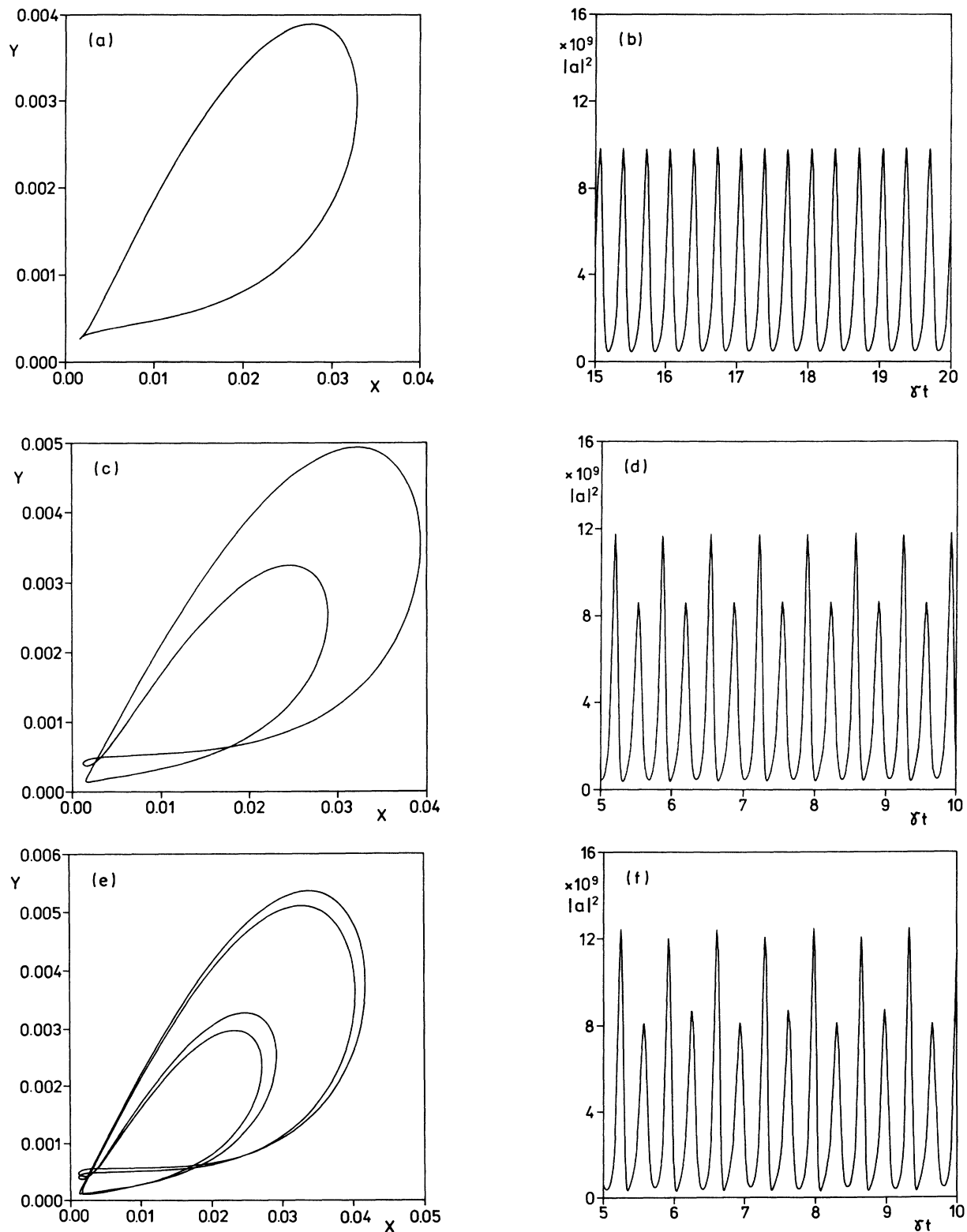


FIG. 2. (a) Phase-space diagram representing the trajectory of the dressed-state laser in the instable region for the parameters chosen along the arrow indicated in Fig. 1. The variables represent the normalized laser intensity $X = |a|^2/N$ and atomic polarization $Y = |S|^2/N^2$. The trajectory represents self pulsing in the form of a 1-cycle. The parameters are $\Omega = 183$, $\Delta_2 = 200$. All other parameters are the same as in Fig. 1. (b) Time dependence of the laser intensity for the 2-cycle solution presented in (a). (c) Same as in (a), but for $\Omega = 181$. The trajectory represents a 2-cycle. (d) Time dependence of the laser intensity for the 2-cycle solution presented in (c). (e) Same as in (a), but for $\Omega = 180$. The trajectory represents a 4-cycle. (f) Time dependence of the laser intensity for the 4-cycle solution presented in (e).

provements of the EHT theory lead typically to small shifts of the boundaries of instabilities. They may therefore in such situations lead to qualitative changes of the asymptotic behavior for parameters very close to thresholds of instabilities. Frequently, in such cases it is enough to improve the theory by going beyond secular approximation and by using EAT [Figs. 6(a) and 6(b)]. EHT theory leads here to self-pulsing, whereas EAT theory as well as the "exact" GET41 both predict stable behavior.

The dramatic breakdown of EHT, and of EAT, occurs in the regions of parameters where the competition of one-photon and two-photon processes takes place. That happens, for instance, in the region far from resonance. Here, however, we present a series of results for $2\Delta_2 \simeq \Omega'$, i.e., not far from the two-photon resonance. In the region where both of these theories predict stable behavior, the

exact theory GET41 predicts self-pulsing behavior with superimposed chaos [Figs. 7(a) and 7(b)]. To understand the physical meaning of this behavior we have calculated the spectrum of emitted radiation. The spectrum is defined via simple Fourier transform of the signal,

$$P(\omega) = \lim_{t \rightarrow \infty} \lim_{T \rightarrow \infty} \frac{1}{T} \left| \int_t^{t+T} e^{i\omega t'} a(t') dt' \right|^2. \quad (5.1)$$

We expect that for such a choice of parameters there will be a strong competition between one-photon and two-photon lasing processes. In fact both one-photon and two-photon EHT predict stable stationary solutions. According to these theories one-photon lasing should occur at the frequency $\Delta_L^{1\text{ph}} \simeq 175$, whereas two-photon

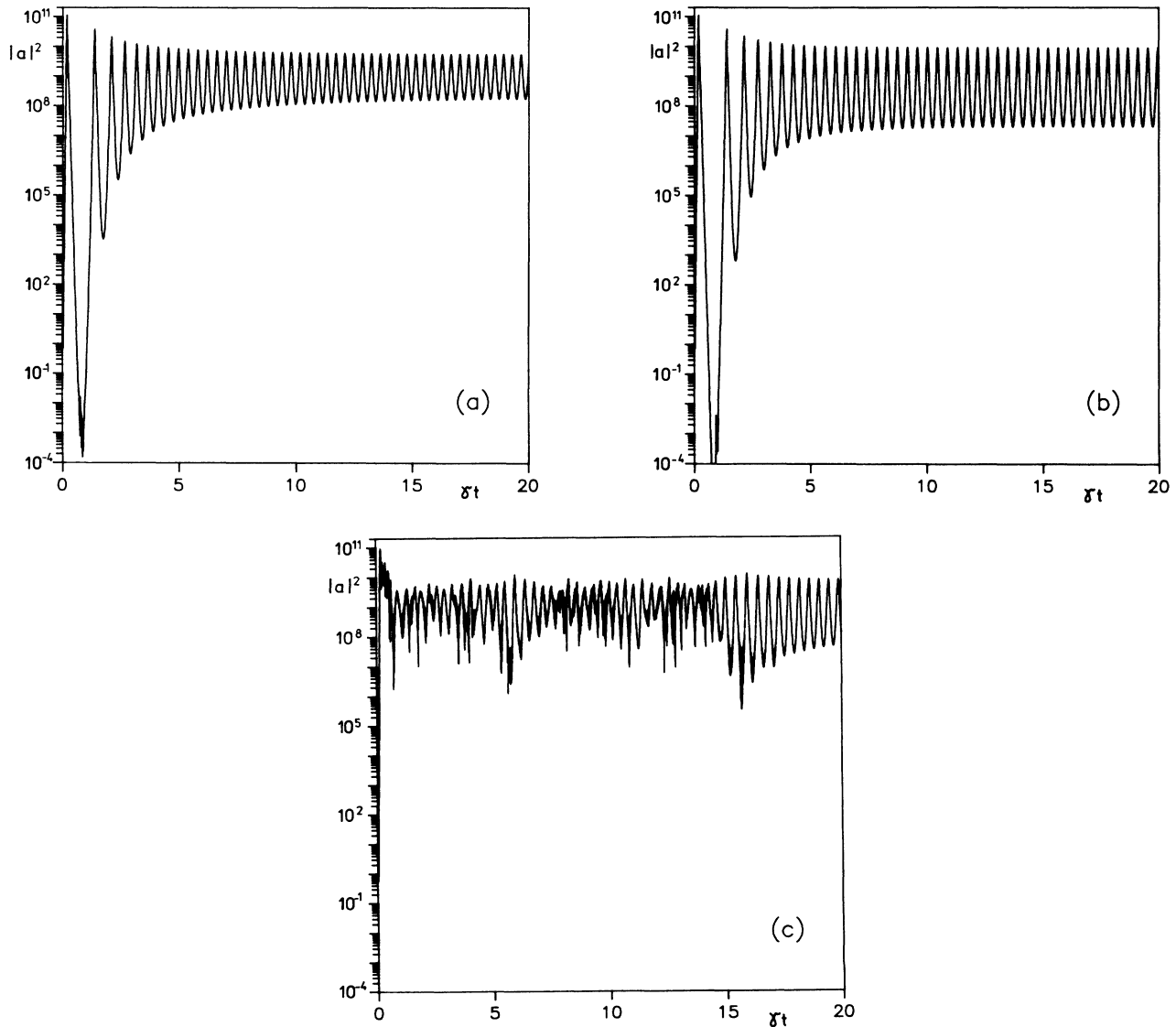


FIG. 3. (a) Time dependence of the laser intensity calculated for the values of $\Omega = \Delta_2 = 300$, and $\Gamma = 100$. All other parameters are chosen as in Fig. 1. The initial value of the cavity field amplitude was $a = 1$. The curve represents the results of the EHT approach. (b) Same as (a), but obtained without the secular approximation, i.e., with the help of the EAT approach. (c) Same as (a), but obtained with the help of the "exact" GET41 approach.

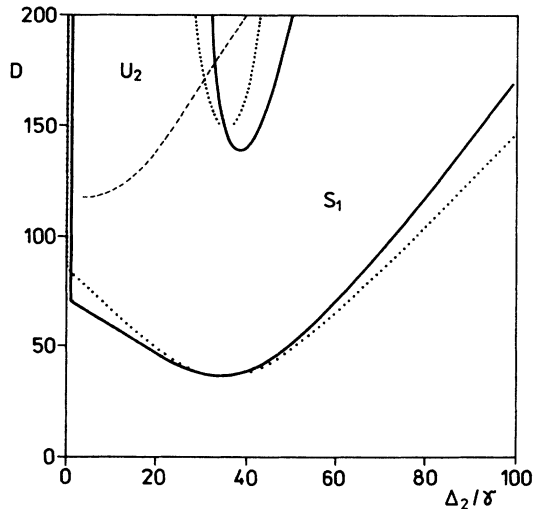


FIG. 4. Regions of stability of stationary mode of operation of one-photon and two-photon dressed-state lasers. The diagram is presented in the D - Δ_2 plane and has been obtained with the help of one- and two-photon versions of EHT theories ($D = g\sqrt{N}$). Full lines are the borders of the stability region given by EHT theory with Bloch-Siegert shifts included. The dotted curves correspond to EHT without Bloch-Siegert shifts (i.e., GET5 theory). Dashed line represent region of existence of the stationary two-photon lasing, as predicted by two-photon version of EHT (this solution is unstable—denoted as U_2). The parameters correspond to those of Ref. [7]: $\Gamma = 15$, $\Delta = -10$, $\Omega = 34$.

lasing at $\Delta_L^{2ph} \simeq 125$. The spectrum of emitted radiation shows characteristic features of both lasing processes, i.e., well-developed peaks close to Δ_L^{1ph} and Δ_L^{2ph} . Additionally we observe a large Rayleigh peak at $\omega = 0$, which indicates the significant role played in the dynamics by multiphoton Rayleigh transitions (i.e., transitions

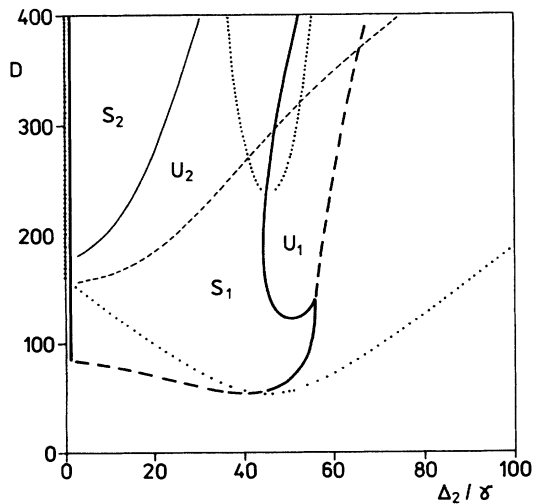


FIG. 5. Same as in Fig. 4, but for slightly larger value of $\Delta_1 = -30$. Note the appearance of the region of stable two-photon action.

between the same kind of dressed states) [Fig. 8(a)]. The same result is presented in logarithmic scale in Fig. 8(b), which shows both lasing peaks more clearly, and continuous background due to the chaotic component of the motion.

Figures 9(a) and 9(b) are obtained in the region where two-photon EHT exhibits self-pulsing and one-photon EHT leads to stable stationary behavior. The full theory GET41 shows, on the other hand, chaos on a full scale [Figs. 9(a) and 9(b)]. The spectrum, calculated from both the one-photon and two-photon EHT theories is

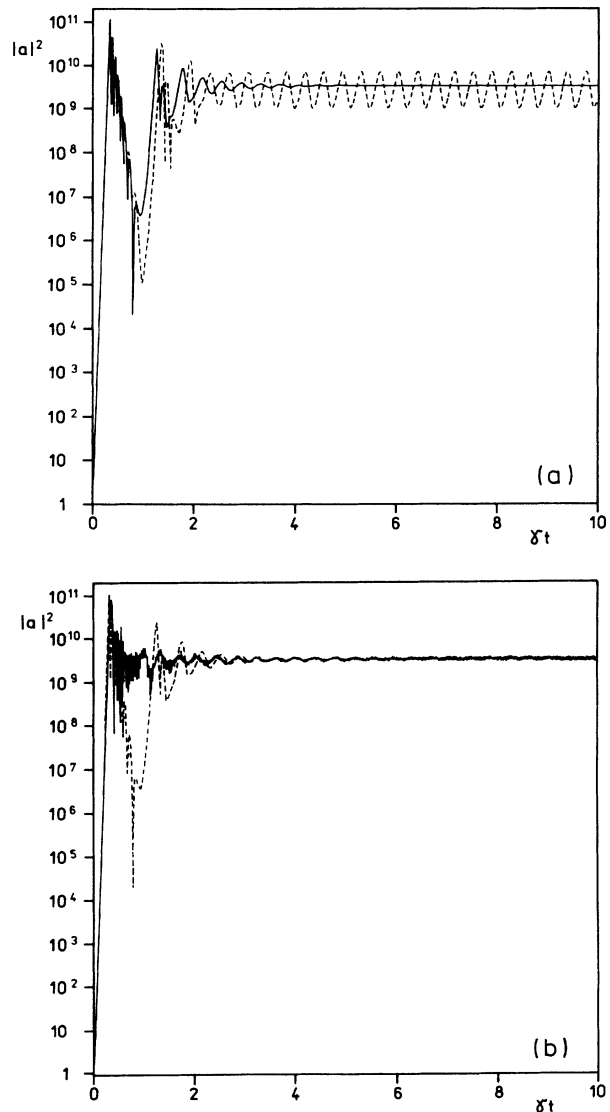


FIG. 6. (a) Time dependence of the one-photon dressed-state laser intensity at the threshold of self-pulsing. The dashed curve represents the result of EHT, the solid curve, the result of EAT. The parameters are $\Omega = 200$, $\Delta_2 = 245$, $\Delta_1 = -100$, $\Gamma = 20$, $g = 0.001$, $N = 3 \times 10^{11}$. (b) Same as (a), but the dashed line represents the result of EAT, whereas the solid represents the “exact” result of GET41.

presented in Fig. 10(a). The spectrum of the two-photon laser exhibits two components: one (close to $\omega = 40$) is located close to the frequency of the unstable stationary solution. The second component of the two-photon laser spectrum ($\omega \simeq 65$) results from self-pulsing, which has roughly the period $T \simeq 2\pi/(65 - 40)$. Note that the second component of the two-photon laser coincides practically with the frequency of one-photon lasing. One can expect that the competition of the two processes is strong. As a result both effective-Hamiltonian theories become invalid. Indeed, the competition between the component of the two-photon laser spectrum due to self-

pulsing, with one-photon lasing leads to fully developed chaotic behavior. To describe this behavior one must use the “exact” GET41 theory. The spectrum calculated from the full theory is broadband and shows complicated structure, characteristic for chaotic behavior.

VI. CONCLUSIONS

We have generalized the theory of the dressed-state laser beyond the effective-Hamiltonian theory (EHT). We have reformulated it in the form of adiabatic elimination taking into account terms neglected in the secular ap-

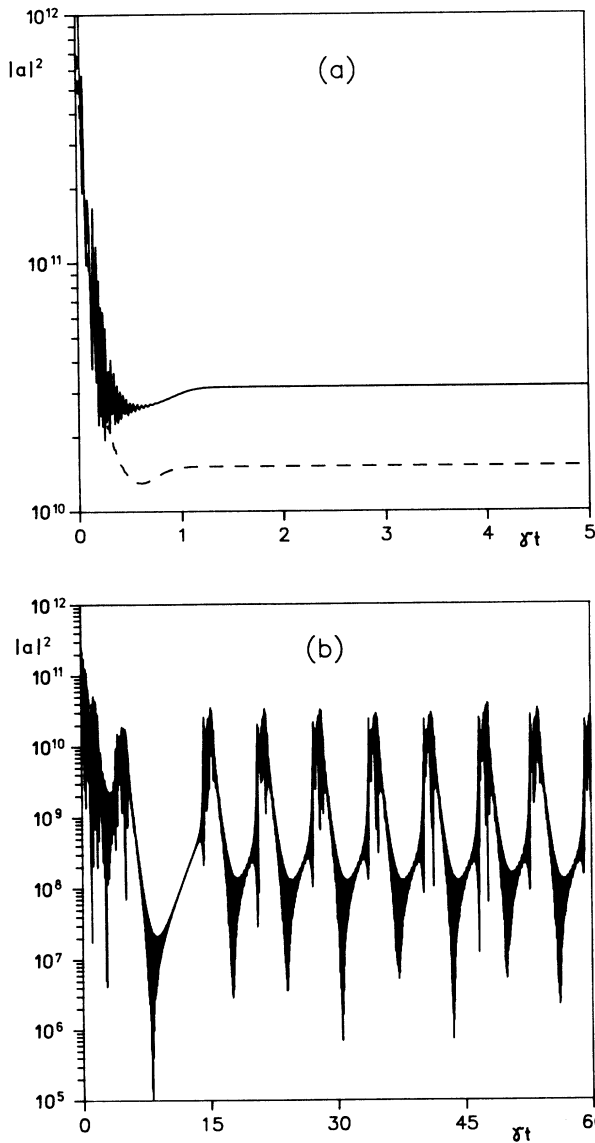


FIG. 7. (a) Time dependence of the dressed-state laser intensity. Both two-photon EAT (solid line) and one-photon EAT (dashed line) predict stable stationary action for the same values of the parameters: $\Omega = 120$, $\Delta_2 = 60$, $\Delta_1 = -100$, $\Gamma = 20$, $g = 0.001$, $N = 3 \times 10^{12}$. (b) Same as (a), but the only presented solid curve represents the “exact” results of GET41.

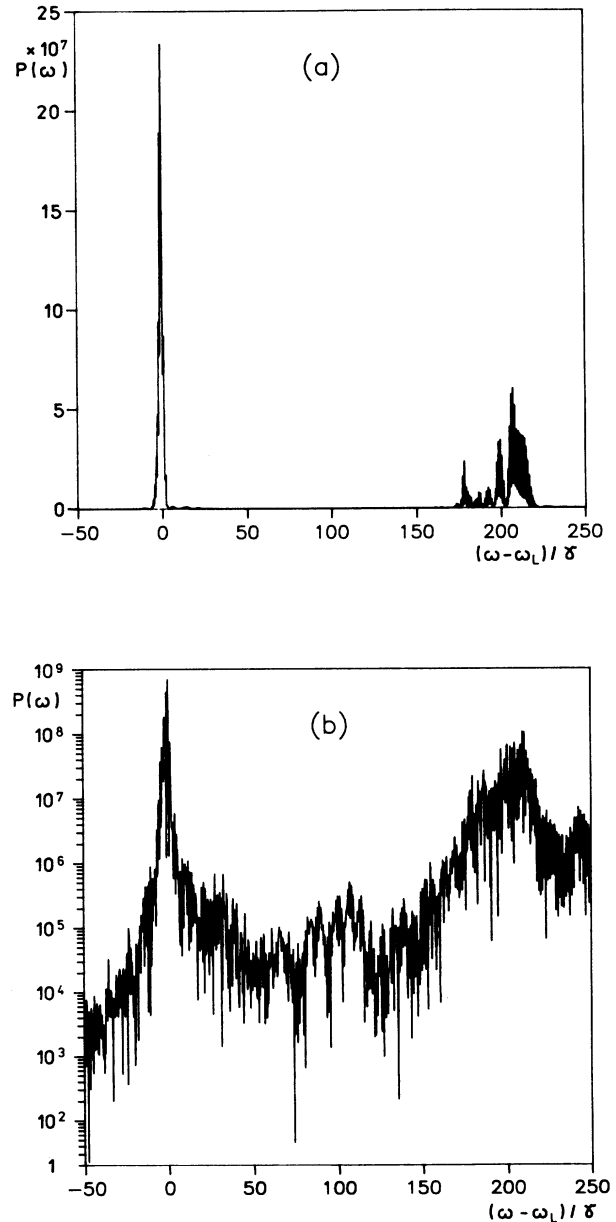


FIG. 8. (a) Spectrum of the laser output (obtained with GET41) $P(\omega)$ for the parameters of Fig. 7. (b) Same as (a), but displayed in logarithmic scale.

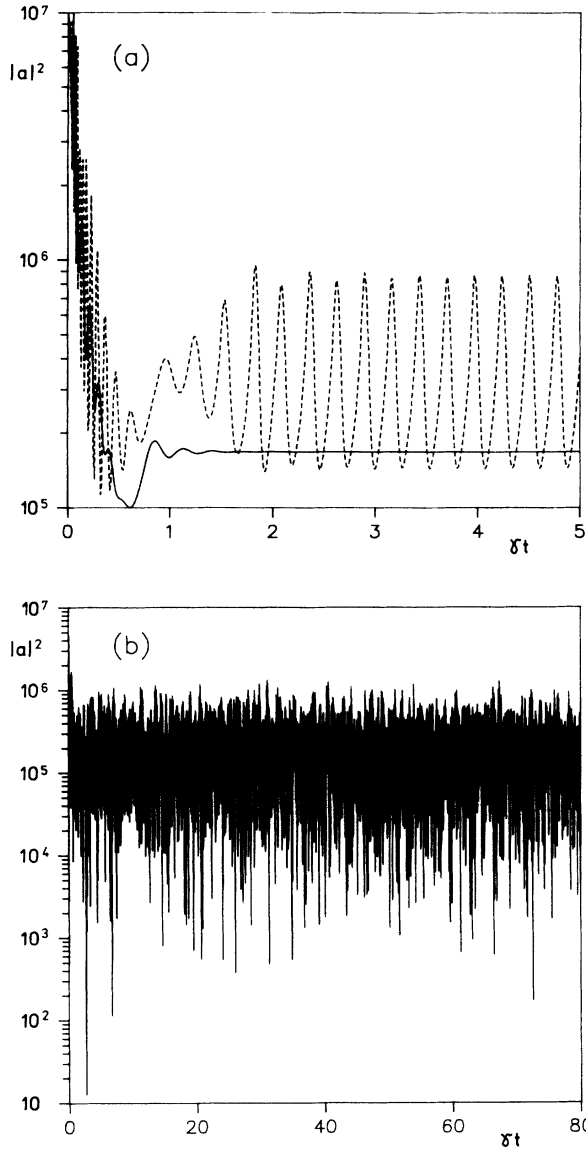


FIG. 9. (a) Time dependence of the dressed-state laser intensity displaying the competition between two-photon self-pulsing and one-photon stationary operation. The dashed curve represents the result of two-photon EAT, the solid curve, the results of one-photon EAT. The parameters are $\Omega = 60$, $\Delta_2 = 30$, $\Delta_1 = -30$, $\Gamma = 15$, $g\sqrt{N} = 350$. (b) Same as (a), but the only presented solid curve represents the "exact" result of GET41.

proximation (EAT). We have also formulated the hierarchy of generalized effective theories (GET) that allow for systematic approximations of the dynamics of dressed-state lasers. The methods presented here can be adopted to other nonlinear optical systems.

We have applied the theory to investigate stability properties of dressed-state lasers in the bad-cavity limit. We have shown that EHT and EAT can be used in principle, when the dressed-state splitting is large enough (i.e., both Ω and Δ_1 should be large). The adiabatic

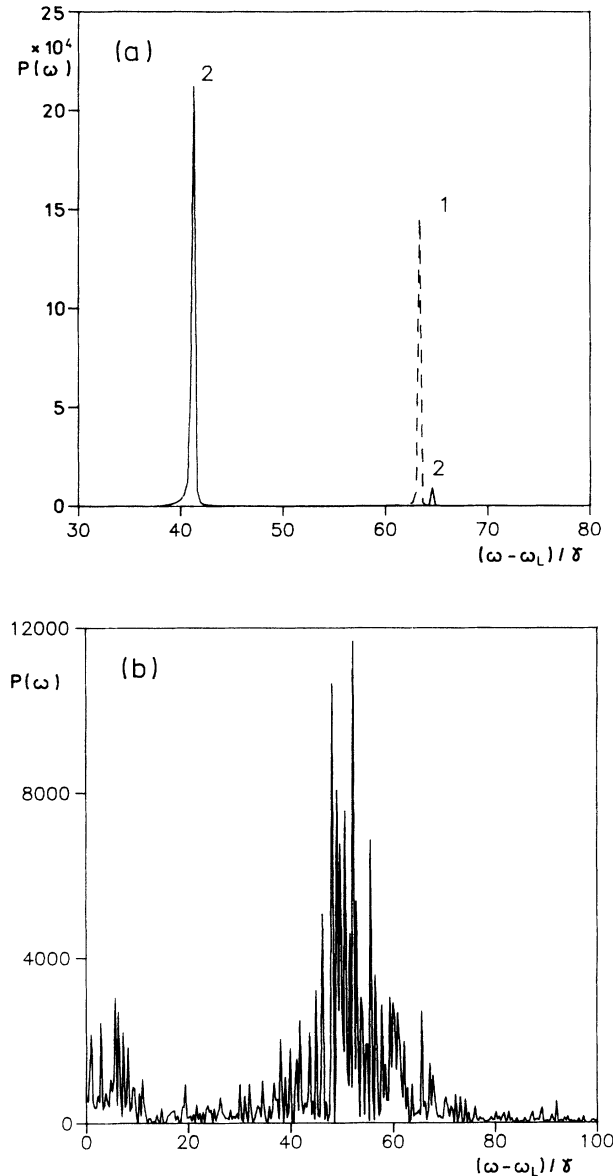


FIG. 10. (a) Spectrum of the laser output $P(\omega)$ for the parameters of Fig. 8. The dashed curve represents the result of two-photon EAT, the solid curve, the results of one-photon EAT. (b) Same as in (a), but the only presented solid curve represents the "exact" result of GET41.

approach breaks down (a) for parameters close to instability threshold; (b) in the presence of strong competition between different kinds of lasing processes.

In the region of validity of EHT, self-pulsing and chaos can be observed, as well as the known routes to chaos. The higher-order instabilities appear in the regions of parameters that lie not too far from the current experimental possibilities [28].

In the region of strong competition between various lasing process, adiabatic theory cannot be used. The out-

put of the laser contains typically chaotic components. The behavior of the system may be analyzed and explained by looking at the spectrum of the emitted radiation.

ACKNOWLEDGMENTS

We acknowledge financial support from a KBN Grant. We thank L. Lugiato for interesting comments.

-
- [1] M. Lewenstein, Y. Zhu, and T. W. Mossberg, *Phys. Rev. Lett.* **64**, 3131 (1990).
- [2] J. Zakrzewski, M. Lewenstein, and T. W. Mossberg, *Phys. Rev. A* **44**, 7717 (1991).
- [3] J. Zakrzewski, M. Lewenstein, and T. W. Mossberg, *Phys. Rev. A* **44**, 7732 (1991).
- [4] J. Zakrzewski, M. Lewenstein, and T. W. Mossberg, *Phys. Rev. A* **44**, 7746 (1991).
- [5] G. S. Agarwal, *Phys. Rev. A* **42**, 686 (1990); *Opt. Comm.* **80**, 37 (1990).
- [6] The experiment with an atomic cell is described in G. Khitrova, J. F. Valley, and H. M. Gibbs, *Phys. Rev. Lett.* **60**, 1126 (1988).
- [7] The experiment with atomic beam is described in A. Lezama, Y. Zhu, M. Kanskar, and T. W. Mossberg, *Phys. Rev. A* **41**, 1576 (1990).
- [8] Y. Zhu, Q. Wu, S. Morin, and T. W. Mossberg, *Phys. Rev. Lett.* **65**, 1200 (1990).
- [9] B. R. Mollow, *Phys. Rev. A* **5**, 2217 (1972).
- [10] F. Y. Wu, S. Ezekiel, M. Ducloy and B. R. Mollow, *Phys. Rev. Lett.* **38**, 1077 (1977).
- [11] R. W. Boyd, M. G. Raymer, P. Narum, and D. J. Harter, *Phys. Rev. A* **24**, 411 (1981).
- [12] C. Cohen-Tannoudji, in *Frontiers of Laser Spectroscopy*, edited by R. Balian, S. Haroche, and S. Liberman, Les Houches, Session XXVII (North-Holland, Amsterdam, 1977); C. Cohen-Tannoudji and S. Reynaud, *J. Phys. B* **10**, 365 (1977).
- [13] D. A. Holm, M. Sargent III, and S. Stenholm, *J. Opt. Soc. Am. B* **2**, 1456 (1985); S. Stenholm, D. A. Holm, and M. Sargent III, *Phys. Rev. A* **31**, 3124 (1985); M. Sargent III and D. A. Holm, *ibid.* **31**, 3112 (1985).
- [14] Y. Zhu, A. Lezama, and T. W. Mossberg, *Phys. Rev. A* **39**, 2268 (1989).
- [15] S. Stenholm, *Phys. Rep.* **6**, 1 (1973); for an alternate method of projection operators see H. Friedman and A. D. Wilson-Gordon, *Opt. Commun.* **24**, 5 (1978).
- [16] L. Allen and J. H. Eberly, *Optical Resonance and Two-level Atoms* (Wiley, New York, 1975).
- [17] For a recent discussion in the context of quantum chaos see for instance R. Graham and M. Höhnerbach, *Phys. Lett.* **101A**, 61 (1984).
- [18] F. Bloch and A. J. F. Siegert, *Phys. Rev.* **57**, 522 (1940).
- [19] See, for instance, H. Haken, *Light*, Vol. 2 of *Laser Light Dynamics* (North-Holland, Amsterdam, 1981); H. Haken, *Laser Theory*, Vol. XXV/2c of *Encyclopedia of Physics*, 2nd corr. ed. (Springer, New York, 1984), and references therein.
- [20] D. Stoler, *Phys. Rev. D* **1**, 3217 (1970); **4**, 1925 (1971); see also *J. Opt. Soc. Am. B* **4** (1987), special issue on *Squeezed States of the Electromagnetic Field*, edited by H. J. Kimble and D. Walls; *J. Mod. Opt.* **34** (1987), special issue on *Squeezed States*, edited by R. Loudon and P. L. Knight.
- [21] R. Bonifacio and L. A. Lugiato, *Lett. Nuovo Cimento* **21**, 510 (1978).
- [22] M. Brambilla, F. Castelli, L. A. Lugiato, F. Prati, and G. Strini, *Opt. Commun.* **83**, 367 (1991); for a unified treatment of optical bistability and multimode lasers see also M. Reid, K. J. McNeil and D. F. Walls, *Phys. Rev. A* **24**, 2029 (1981).
- [23] B. Ségard and B. Macke, *Phys. Rev. Lett.* **60**, 412 (1988); B. Ségard, B. Macke, L. A. Lugiato, F. Prati, and M. Brambilla, *Phys. Rev. A* **39**, 703 (1989).
- [24] D. Grandclément, G. Grynberg, and M. Pinard, *Phys. Rev. Lett.* **59**, 40, 44 (1987).
- [25] See, for instance, G. S. Agarwal, *Quantum Statistical Theories of Spontaneous Emission*, Springer Tracts in Modern Physics 70 (Springer-Verlag, Berlin, 1974).
- [26] G. Grynberg, N. Pinard, and P. Verkerk, *J. Phys.* **47**, 617 (1986).
- [27] C. Cohen-Tannoudji, J. Dupont-Roc, and G. Grynberg, *Processus d'Interaction Entre Photons et Atomes* (Savoirs Actuels, Inter Editions/Editions du CNRS, Paris, 1988).
- [28] Recently two-photon cw dressed-state lasing has been observed by D. J. Gauthier, Q. Wu, S. E. Morin, and T. W. Mossberg (unpublished). These authors also observed oscillatory behavior of the laser.